Ab initio studies of the nuclear magnetic resonance chemical shifts of a rare gas atom in a zeolite

Cynthia J. Jameson and Hyung-Mi Lim
Department of Chemistry, University of Illinois at Chicago, 845 W. Taylor St., Chicago, Illinois 60607-7061

(Received 20 April 1995; accepted 6 June 1995)

The intermolecular chemical shift of a rare gas atom inside a zeolite cavity is calculated by *ab initio* analytical derivative theory using gauge-including atomic orbitals (GIAO) at the Ar atom and the atoms of selected neutral clusters each of which is a 4-, 6-, or 8-ring fragment of the zeolite cage. The Si, Al, O atoms and the charge-balancing counterions (Na^+, K^+, Ca^{2+}) of the clusters (from 24 to 52 atoms) are at coordinates taken from the refined single crystal x-ray structure of the Na*A*, K*A*, and Ca*A* zeolites. Terminating OH groups place the H atom at an appropriate O–H distance along the bond to the next Si or Al atom in the crystal. The chemical shift of the Ar atom located at various positions relative to the cluster is calculated using Boys–Bernardi counterpoise correction at each position. The dependence of the rare gas atom chemical shift on the Al/Si ratio of the clusters is investigated. The resulting shielding values are fitted to a pairwise additive form to elicit effective individual Ar–O, Ar–Na, Ar–K, Ar–Ca intermolecular shielding functions of the form $\sigma(^{39}\mathrm{Ar, Ar\cdots O_{zeol}})=a_6r^{-6}+a_8r^{-8}+a_{10}r^{-10}+a_{12}r^{-12}$, where r is the distance between the Ar and the O atom. A similar form is used for the counterions. The dependence of the Ar shielding on the Al/Si ratio is established (the greater the Al content, the higher the Ar chemical shift), which is in agreement with the few experimental cases where the dependence of the ^{129}Xe chemical shift on the Al/Si ratio of the zeolite has been observed. © *1995 American Institute of Physics.*

INTRODUCTION

The extremely high sensitivity of the ^{129}Xe NMR chemical shift to its environment has made the Xe atom a widely used probe of the structure of zeolites,[1–3] polymers,[4–6] graphite,[7] coals,[8] and other materials.[9,10] In particular, the applications of Xe NMR spectroscopy to the investigation of the structure of zeolites has been the subject of a large number of publications, and those prior to 1991 have been reviewed.[3] The ^{129}Xe chemical shift has been taken as an indicator of pore size,[11–15] cation distribution,[16,17] and distribution of metal atoms.[18] An understanding of the sensitivity of the chemical shift to these parameters, crucial to the quantitative application of the empirical observations, still remains elusive.

The observations of the chemical shifts of individual clusters Xe_n in type *A* zeolites has permitted the investigation of the Xe–Xe contributions to the chemical shifts in these cages. The incremental shifts with increasing *n* and the temperature dependence of the cluster shifts have been reproduced by grand canonical averaging.[19] In these theoretical simulations, the nuclear shielding of the rare gas atom is assumed to be pairwise additive and the ^{129}Xe intermolecular shielding function for the Xe–Xe interaction was derived from the *ab initio* intermolecular shielding function of ^{39}Ar in Ar–Ar. The latter had been found to reproduce reasonably well the intermolecular chemical shifts of ^{129}Xe nuclei in mixtures of Xe–Xe, Xe–Kr, and Xe–Ar in the gas phase, including their temperature dependence.[20] In other words, the Xe–Xe contributions to the ^{129}Xe chemical shift within the alpha cages is assumed to be the same as that in the dilute Xe gas, only the distribution of Xe–Xe distances in the Xe_n clusters in type *A* zeolites is different. In these simulations, the intermolecular chemical shift contributions from the Xe–zeolite framework interactions were approximated by pairwise-additive contributions from oxygen and Na ions in the appropriate positions in the lattice, as derived from the refined x-ray structure of dehydrated zeolite Na*A*. The xenon atoms are exposed primarily to these components of the zeolite, so that any contributions from the Si and Al atoms of the framework were taken to be represented by the effective contributions from the oxygen atoms. The potential energy was likewise treated in a similar pairwise-additive sum. For the ^{129}Xe chemical shifts contributed by the effective oxygens, a simple model *ab initio* ^{39}Ar in Ar–OH_2 shielding surface was scaled up to ^{129}Xe in Xe–OH_2. Likewise the ^{129}Xe chemical shift contribution from the Na ions was modeled from the *ab initio* ^{39}Ar shielding function in the Ar–Na^+ system.[20] The grand canonical average obtained with these shielding functions fortuitously reproduced the observed ^{129}Xe chemical shift of a single Xe atom in the alpha cage.[19] That the increments between the Xe_n cluster shifts were well-reproduced, including their temperature dependence, might have been expected from the good agreement found in the gas phase chemical shifts based on the same *ab initio* derived Xe–Xe intermolecular chemical shift function, since these chemical shift increments are largely due to the Xe–Xe interactions. On the other hand, the good agreement with the ^{129}Xe chemical shift of a single Xe atom in the alpha cage could have been fortuitous. Modeling the O atoms in the zeolite with O in OH_2 and the Na ion in the zeolite by a bare Na^+ ion is clearly too simplistic. There is no systematic way of improving this model so as to be able to apply it to the chemical shift of a Xe atom in various zeolites of differing Al/Si ratio, for example. In this paper, we present *ab initio* calculations of the effects of a zeolite framework on the

NMR chemical shift of a rare gas atom, including the changes in the Al/Si ratio.

In the limit of zero Xe coverage, the ^{129}Xe NMR chemical shift has been observed to be sensitive to the structure of a zeolite, to its pore size,[11–15] to its Al/Si ratio,[21] and to the size and types of the cations that balance the charge in the aluminated zeolites.[16,17] In the limit of zero Xe coverage, the only contributions to the chemical shift are the Xe–zeolite interactions. The temperature dependence and the magnitude of this chemical shift is affected by the averaging, in fast exchange, over all possible positions that the Xe atom takes, that is, an appropriate weighting of the various points on the ^{129}Xe shielding function corresponding to these positions. The large changes in the chemical shifts that are observed upon cation exchange in a faujasite of a fixed Al/Si ratio have been carefully quantitatively studied recently.[16] The change in the ^{129}Xe chemical shift in ZSM-5 upon variation of the Al/Si ratio has also been properly documented recently.[21] These intriguing trends are more demanding of a model for rare gas atom–zeolite intermolecular chemical shifts than can be provided by shielding calculations in the Ar–OH_2 and Ar–Na^+ bare ion model systems.

Even when the Al/Si ratio of the zeolite is well-established, the distributions of the framework Al atoms are not usually well known. The distribution and locations of counterions in zeolites are also not completely known, even in the well-studied faujasites. In contrast, in the *A*-type zeolites such as Na*A*, K*A*, and Ca*A*, single crystal x-ray refinement of the dehydrated zeolite has unequivocally located every Si and Al position as well as the positions of the cations.[22–24] The *A* zeolites provide a good starting point for a theoretical investigation of the shielding of a rare gas atom occluded within a zeolite, for only in these zeolites have we observed the individual chemical shifts of Xe_n clusters, $n=1$ to 8 in Na*A* and $n=1-4$ in K*A*,[25,26] which can provide excellent critical tests of individual averaging in a single alpha cage where all the framework atoms and the counterions are at well-known locations. Therefore, we begin with representing the *A*-type zeolite framework with fragments containing 4, 6, and 8 T (Al or Si) atoms made neutral with the appropriate number of Na^+ or K^+ ions. We use the actual coordinates of the T, O, and cations based on x-ray data on dehydrated Na*A* and K*A* zeolite.[22,23] In addition we consider the zeolite Ca*A* fragments in which the positions of the framework atoms and the Ca^{2+} have also been determined.[24] The response of the ^{39}Ar shielding to these zeolite fragments, calculated by *ab initio* techniques using gauge-including-atomic orbitals (GIAO) is our model for the intermolecular chemical shift of a rare gas atom due to its interactions with a zeolite. Furthermore, we successively replace the Al atoms in these fragments with Si and find that the shielding response of the Ar atom changes with Al/Si ratio of the fragment.

COMPUTATIONAL METHODS

Ab initio calculations

In the theory of NMR chemical shifts there are two perturbing magnetic fields, one due to the homogenous external field and the other is due to the magnetic moment of the nucleus. The Hamiltonian of an atom or molecule in a magnetic field does not contain the magnetic field itself but rather its magnetic vector potential. The latter is not uniquely determined, but only determined up to the gradient of an arbitrary gauge function. The nuclear magnetic shielding is independent of this gauge function, of course, but only if a complete basis set is used in the calculations. The coupled Hartree–Fock (CHF) or random phase approximation (RPA) methods have been used in conventional calculations of nuclear shielding with a common gauge origin, usually at the center of charge of the molecule. These shielding calculations have been shown to be sensitive to the choice of gauge origin even when using extended basis sets, because they result from taking the sum of two large numbers with opposite signs, of which one is easily obtained very accurately (the diamagnetic contribution) the other rather inaccurately (the paramagnetic contribution). Therefore, various techniques have been devised to minimize the gauge-origin-related errors associated with using an incomplete basis set of functions.[27] The most commonly used methods are individual gauge for localized orbitals (IGLO) developed by Schindler and Kutzelnigg,[28,29] where an individual gauge origin is chosen for each localized molecular orbital, localized orbitals at local origins (LORG) developed by Hansen and Bouman,[30] and the gauge-including atomic orbitals (GIAO), in which a gauge factor is applied to each atomic orbital basis function, originally developed by Ditchfield[31] and adapted to the analytic gradients approach and more efficient algorithms by Pulay.[32] We have used the LORG approach and its second order electron correlation version (SOLO) in earlier work, and the GIAO method for the same systems.[33] In this paper we report only results from GIAO calculations.[34]

We describe the method only very briefly. For details, the original paper[32] and a recent review[35] should be consulted. The basis functions used explicitly depend on the external homogeneous magnetic field by applying a gauge factor $\exp[-i(\mathbf{B}\times\mathbf{R}_p)\cdot\mathbf{r}/2c]$ to every Gaussian basis function centered at $\mathbf{R}_p$. These are called gauge-including atomic orbitals. The gauge factor can be absorbed in the coordinates of the orbital centers $\mathbf{R}_p$. The latter then become complex and magnetic field dependent. In analogy with *ab initio* gradient theory where the basis function centers depend on the nuclear positions, the basis functions in the GIAO method are twisted around the z axis (the field direction) in the imaginary xy plane. The basis for the efficient implementation of the GIAO method is the close mathematical relationship to the analytic gradient theory for calculations of force constants. The intrinsic advantage of the method is that GIAOs are exact first order wave functions of the one-center problem in the presence of a magnetic field. The shielding is expressed in the usual relation in terms of the first-order reduced density matrix in the AO basis and the matrix of the one-electron part of the Hamiltonian, except that here the matrices are in terms of the field-dependent basis functions. The coupled perturbed Hartree–Fock procedure is performed in the AO basis, thereby eliminating the necessity for the 4-index transformation of the two-electron integrals. The ne-

glect of small integrals which do not contribute significantly to the final results invokes the uncoupled Hartree–Fock approximation to estimate the contribution of an integral before it is calculated. The code TX90 implemented on an IBM RS/6000 was generously provided by Pulay.[34]

Our model system is an argon atom in the presence of a portion of the zeolite cage, represented by a neutral fragment. The zeolite fragments used in this work are 4-rings, 6-rings, and 8-rings with the following formulas:

4-ring: $[Si_2Al_2O_4(OH)_8]^{2-}Na_2^+$,

6-ring: $[Si_3Al_3O_6(OH)_{12}]^{3-}Na_3^+$,

8-ring: $[Si_4Al_4O_8(OH)_{16}]^{4-}Na_4^+$,

where the Si, Al, O atoms are all located at the coordinates taken from the single-crystal x-ray refinement of dehydrated Na*A*.[22] The H atoms are located on a line joining the O atom to the appropriate Si or Al atom in the x-ray structure, with an appropriate O–H bond length (0.958 Å). The counterions, Na^+ in this case, are also located at positions dictated by the x-ray structure, the choices being sites of type I, II, or III. The K*A* zeolite fragments are likewise represented by rings of the same composition, where the atoms are located at the coordinates taken from the x-ray refinement of dehydrated K*A*, with the K^+ ions in the appropriate K*A* x-ray structure in sites of type I, I′, II, III, III′.[23] The types of positive ion sites used to balance the charge of the fragments are taken such as to represent statistically the actual distribution in an alpha cage, which for Na^+ ion is 8:3:1 of sites I, II, and III, respectively.

Calculations were also done for an Ar atom in the presence of 4-rings and 6-rings of varying Al/Si ratio

$[Si_4O_4(OH)_8]$,

$[Si_3AlO_4(OH)_8]^-Na^+$

for comparison with $[Si_2Al_2O_4(OH)_8]^{2-}$ Na_2^+ and

$[Si_6O_6(OH)_{12}]$,

$[Si_5AlO_6(OH)_{12}]^-Na^+$,

$[Si_4Al_2O_6(OH)_{12}]^{2-}Na_2^+$

for comparison with $[Si_3Al_3O_6(OH)_{12}]^{3-}Na_3^+$. Furthermore, we carried out *ab initio* shielding calculations on Ar in the presence of the neutral fragment of a joined 4- and 6-ring,

$[Si_4Al_4O_9(OH)_{14}]^{4-}Ca_2^{2+}$

which will serve as a model for the intermolecular shielding of a rare gas atom in Ca*A*. Here, too, the coordinates of Si, Al, O, and Ca^{2+} are taken from the actual positions obtained from the x-ray data[24] and the terminating hydrogens are on the line to the Si or Al framework position, at an appropriate O–H distance. The typical fragments used in this work are shown in Figs. 1–4, although we also carried out calculations on fragments with the counterions in various other crystallographic positions.

It is well known that the accuracy of NMR shielding calculations depends upon the quality of the basis sets used, even when local origins are used,[27,29,30] and in the GIAO method.[32,35] For the second-row elements (such as Ar) at least two sets of polarization functions within a triple-zeta basis set are required to reach convergence at the SCF level.[27,29] We use a 6311G** Pople basis set augmented by three sets of *d*-type polarization functions for the Ar atom. The basis sets used here for Al, Si, and O were the Pople 3-21G set and the Na^+ ion and K^+ (and Ca^{2+}) ion functions were taken from Huzinaga[36] $[7s4p]$ contracted to (43/4) and $[9s6p]$ contracted to (333/33), respectively. The calculation therefore involves using a locally dense basis at Ar compared to the zeolite fragment. The use of locally dense basis func-

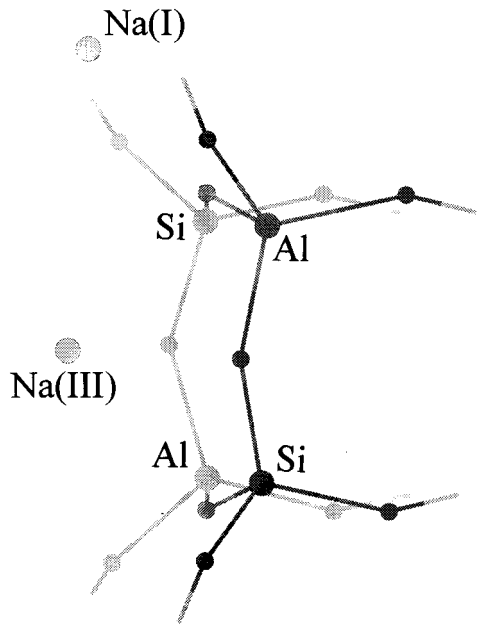

FIG. 1. A portion of the Na*A* zeolite cage is represented by a neutral fragment which is a 4-ring with the formula: $[Si_2Al_2O_4(OH)_8]^{2-}Na_2^+$.

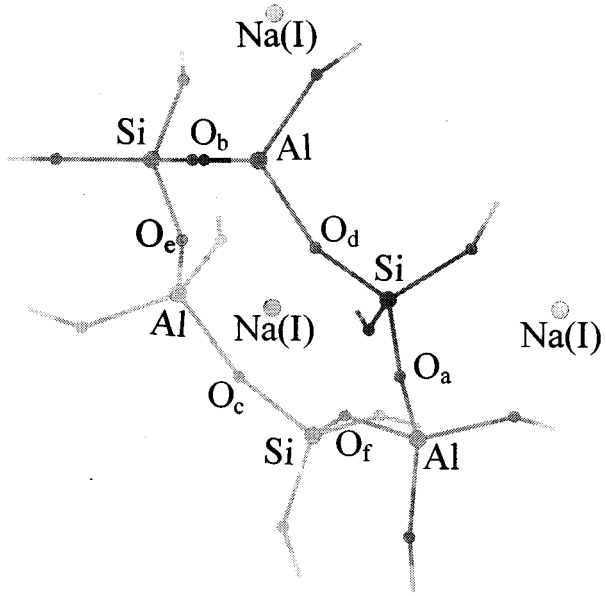

FIG. 2. A portion of the Na*A* zeolite cage is represented by a neutral fragment which is a 6-ring with the formula: $[Si_3Al_3O_6(OH)_{12}]^{3-}Na_3^+$. The labels a–f on the O atoms will be used in the discussion of Al/Si ratio.

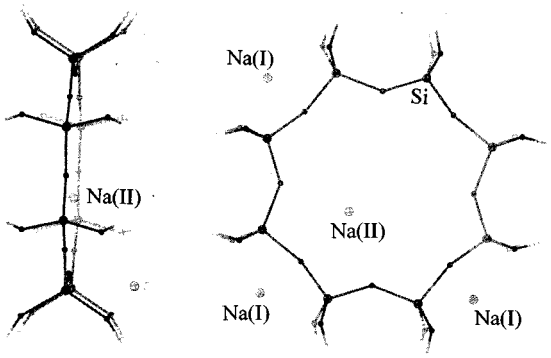

FIG. 3. A portion of the Na*A* zeolite cage is represented by a neutral fragment which is a 8-ring with the formula: $[Si_4Al_4O_8(OH)_{16}]^{4-}Na_4^+$.

tions at the nucleus for which the shielding is being calculated has been proposed and extensively tested by Chesnut.[37,38] The Ar basis must be large enough to get good shielding response at the ^{39}Ar nucleus at short and long distances from the zeolite fragment. Polarization functions are very important in this respect. The atoms of the zeolite fragment do not need as large a basis set since their shieldings are not being calculated, and we used a compromise size so that the same size basis is used for all the fragments in this work.

The problem of basis set superposition errors (BSSE) is of great importance not just in calculating interaction energies but also molecular electronic properties. The problem of BSSE, an explanation of its origin, and the methods of circumventing it have been reviewed.[39,40] BSSE in intermolecular shielding calculations is important since polarization functions and functions with diffuse exponents which are employed in shielding calculations are readily used by all monomers in the complex and yield BSSE of the same order of magnitude as the interaction energy itself. The purpose of a good BSSE correction scheme is to yield the true interaction energy (or molecular electronic property) corresponding to the quality of the basis set and the method of calculation. A standard approach to circumvent BSSE problems consists in the application of the counterpoise method (CP) by Boys and Bernardi.[41] Each subsystem (monomer) is to be calculated in the complete basis of the supersystem. The monomer (free Ar atom) shieldings to be used are calculated in the full supersystem (Ar plus zeolite fragment) basis. This is the so-called full counterpoise method (FCP). In these systems the BSSE in the ^{39}Ar shieldings is a function of position of the Ar with respect to the fragment and is of the order of a few ppm. Altogether 164 GIAO calculations were carried out for one Ar atom in the presence of various neutral zeolite fragments in this work; each calculation is done with full counterpoise correction.

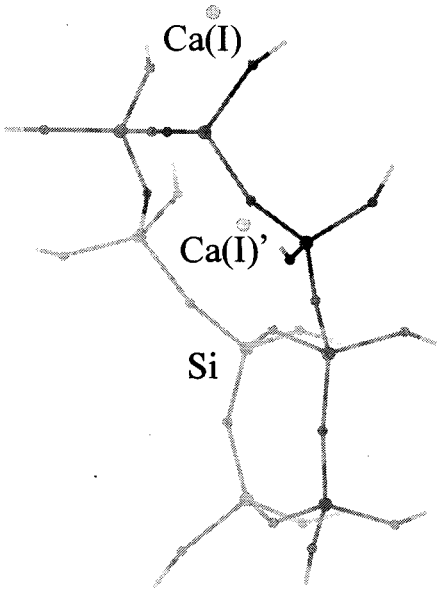

FIG. 4. A portion of the Ca*A* zeolite cage is represented by a neutral fragment of a joined 4- and 6-ring with the formula: $[Si_4Al_4O_9(OH)_{14}]^{4-}$ Ca_2^{2+}.

The effective intermolecular shielding functions, $\sigma(^{39}\mathrm{Ar}, \mathrm{Ar}\cdots\mathrm{O_{zeol}})$ and $\sigma(^{39}\mathrm{Ar}, \mathrm{Ar}\cdots\mathrm{M_{zeol}})$, M=Na$^+$, K$^+$, Ca^{2+}

The Ar atom is placed at various positions relative to the Na*A* fragments, chosen so as to elicit the desired ''effective'' shielding functions $\sigma(^{39}\mathrm{Ar},\ \mathrm{Ar}\cdots\mathrm{O_{zeol}})$ and $\sigma(^{39}\mathrm{Ar},\ \mathrm{Ar}\cdots\mathrm{Na_{zeol}})$. The *ab initio* value of the ^{39}Ar shielding at various positions relative to the various 4-ring, 6-ring, and 8-ring fragments are fitted to a pairwise additive sum

$$\sigma(^{39}\mathrm{Ar},\ \mathrm{Ar}\cdots\mathrm{ring}) = \Sigma_i \sigma(^{39}\mathrm{Ar},\ \mathrm{Ar}\cdots\mathrm{O}_i) + \Sigma_j \sigma(^{39}\mathrm{Ar},\ \mathrm{Ar}\cdots\mathrm{Na}_j).$$

The oxygen atoms for zeolite fragments with Al/Si ratio=1.0 were all assumed to have the same (average) contribution to the $\sigma(^{39}\mathrm{Ar},\mathrm{Ar}\cdots\mathrm{O_{zeol}})$ shielding function, even though there are actually four types of oxygen sites in this *A*-type zeolite. Similarly, all three types of Na^+ sites were assumed to have the same (average) contribution to the $\sigma(^{39}\mathrm{Ar},\mathrm{Ar}\cdots\mathrm{O_{zeol}})$ shielding function.

A grid of points parallel to the ring is chosen, taking into account that since the Al, Si, and H atoms are not being represented in the fitting, the *ab initio* calculations do not place the Ar close to Al, Si, or H. This grid is moved to selected distances from the ring from 2 Å up to 6 Å. The shielding functions are taken to be of the form

$$\sigma(^{39}\mathrm{Ar},\ \mathrm{Ar}\cdots\mathrm{O_{zeol}}) = a_6 r^{-6} + a_8 r^{-8} + a_{10} r^{-10} + a_{12} r^{-12},$$

$$\sigma(^{39}\mathrm{Ar},\ \mathrm{Ar}\cdots\mathrm{Na_{zeol}}) = b_6 r^{-6} + b_8 r^{-8} + b_{10} r^{-10} + b_{12} r^{-12},$$

and

$$\sigma(^{39}\mathrm{Ar},\ \mathrm{Ar}\cdots\mathrm{K_{zeol}}) = c_6 r^{-6} + c_8 r^{-8} + c_{10} r^{-10} + c_{12} r^{-12},$$

based on our previous experience with the distance dependence of intermolecular shielding functions.[20,42,43]

The *ab initio* values for all the Na*A* and K*A* fragments are all fitted together in a linear least squares procedure to

obtain the parameters a_k, b_k, and c_k for zeolite fragments with Al/Si ratio=1.0. In this way, the above three shielding functions are obtained. Similarly, the $\sigma(^{39}\mathrm{Ar}, \mathrm{Ar}\cdots\mathrm{Ca}_{\mathrm{zeol}})$ shielding function was obtained for the Ca*A* zeolite fragment with Al/Si=1.0 from the fitting to the *ab initio* values for the joined 4- and 6-ring fragment, $[\mathrm{Si}_4\mathrm{Al}_4\mathrm{O}_9(\mathrm{OH})_{14}]^{4-}\ \mathrm{Ca}_2^{2+}$ using the already known $\sigma(^{39}\mathrm{Ar}, \mathrm{Ar}\cdots\mathrm{O}_{\mathrm{zeol}})$ for the system with Al/Si ratio=1.0. This result and the separate fitting of the joined 4- and 6-ring fragment to $\sigma(^{39}\mathrm{Ar},\mathrm{Ar}\cdots\mathrm{O}_{\mathrm{zeol}})$ and $\sigma(^{39}\mathrm{Ar}, \mathrm{Ar}\cdots\mathrm{Ca}_{\mathrm{zeol}})$ were found to be indistinguishable from fitting all the results from the Na*A*, K*A*, and Ca*A* fragments together.

Since the Si and Al atoms are not included in fitting to the sums of atomic contributions to the ^{39}Ar shielding, the oxygen contribution $\sigma(^{39}\mathrm{Ar}, \mathrm{Ar}\cdots\mathrm{O}_{\mathrm{zeol}})$ is an effective shielding function which describes the effect of the entire framework (not including the cations). The bent T–O–T arrangements in zeolites ensures that adsorbed species get close only to oxygen atoms, with the Si and Al relatively farther away. The intermolecular shielding is a consequence of overlap compression and exchange, with much smaller contributions from dispersion.[20] Therefore, it is probably justified to fit the entire calculated shielding to contributions from oxygen atoms and cations only. We also examined the fit to inverse powers -4, -6, -8, -10.

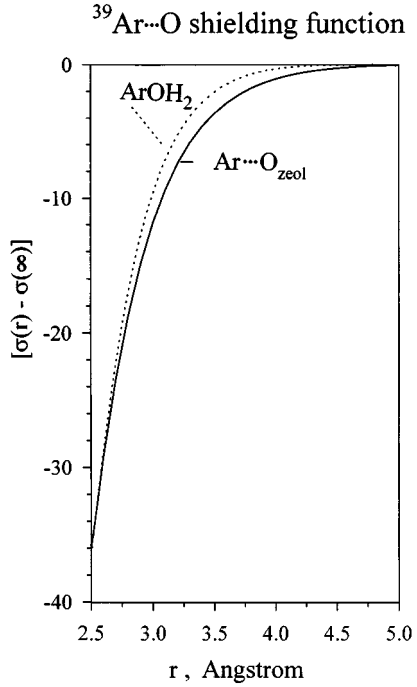

FIG. 5. The shielding function $\sigma(^{39}\mathrm{Ar}, \mathrm{Ar}\cdots\mathrm{O}_{\mathrm{zeol}})$ for the zeolite fragments with Al/Si ratio=1.0, obtained from fitting to the *ab initio* values of ^{39}Ar shielding for Na*A*, K*A*, and Ca*A* fragments.

RESULTS AND DISCUSSIONS

The ^{39}Ar shielding function in Ar···O_{zeol}

If we assume that the $\sigma(^{39}\mathrm{Ar}, \mathrm{Ar}\cdots\mathrm{O}_{\mathrm{zeol}})$ function is the same for all *A*-type frameworks with Al/Si ratio=1.0, then the fitting of all the *ab initio* values for the Na*A*, K*A*, and Ca*A* zeolite fragments together leads to a common oxygen atom contribution to the ^{39}Ar shielding function, $\sigma(^{39}\mathrm{Ar}, \mathrm{Ar}\cdots\mathrm{O}_{\mathrm{zeol}})$, for all three zeolites. On the other hand, it is also possible to consider that zeolites Na*A* and K*A* both having monovalent counterions, could be represented by a common oxygen atom contribution to the ^{39}Ar shielding function, whereas the *A* zeolites with divalent cations could have a different $\sigma(^{39}\mathrm{Ar}, \mathrm{Ar}\cdots\mathrm{O}_{\mathrm{zeol}})$ function. By using the results from the former, we ensure that the shielding functions for the cation contributions $\sigma(^{39}\mathrm{Ar}, \mathrm{Ar}\cdots\mathrm{Na}_{\mathrm{zeol}})$, $\sigma(^{39}\mathrm{Ar}, \mathrm{Ar}\cdots\mathrm{K}_{\mathrm{zeol}})$, and $\sigma(^{39}\mathrm{Ar}, \mathrm{Ar}\cdots\mathrm{Ca}_{\mathrm{zeol}})$, are directly comparable to each other. The shielding function $\sigma(^{39}\mathrm{Ar}, \mathrm{Ar}\cdots\mathrm{O}_{\mathrm{zeol}})$ for the zeolite fragments with Al/Si ratio=1.0 is shown in Fig. 5 together with the Ar–OH_2 shielding function used previously.[19] There is a pronounced difference between using a realistic zeolite fragment and a water molecule to represent the oxygen contributions to the shielding of the rare gas atom. The oxygen contributions (per oxygen atom) to the intermolecular shielding of ^{39}Ar from zeolite *A* fragments are greater than the contributions from the O atom in the Ar···OH_2 system. Our previous models for Ar shielding in the Ar···zeolite interaction provided incorrect relative contributions from the O and Na atoms, although arriving at a total shielding that was in good agreement with experiment for the ^{129}Xe shielding of a single Xe atom in an alpha cage.[19]

The ^{39}Ar shielding function in Ar···Na_{zeol}, in Ar···K_{zeol}, and in Ar···Ca_{zeol}

One important finding from this work is to verify that the shielding response of the rare gas atom to the Na^+ ion in the zeolite fragment is not qualitatively the same as its response to an isolated Na^+ ion. In Fig. 6, we compare $\sigma(^{39}\mathrm{Ar}, \mathrm{Ar}\cdots\mathrm{Na}_{\mathrm{zeol}})$ to the previously published ^{39}Ar shielding in the Ar···Na^+ bare ion system. The long tail of the ^{39}Ar shielding in the presence of the bare Na^+ ion, already discussed in Ref. 42, is not found in the ^{39}Ar shielding in the Ar···zeolite fragment. This clearly shows that the Na^+-in-zeolite evokes a shielding response from the rare gas atom which is distinctly different from the shielding response evoked by an isolated (''bare'') positive ion. This is in agreement with the previous finding that the functional form of the distance dependence of the ^{39}Ar shielding in Ar···NaH is qualitatively different from the distance dependence of the ^{39}Ar shielding in Ar···Na^+.[42] The assumption that the counterions in the zeolite behave like independent ions, widely used in the interpretation of isosteric heats and adsorption isotherms of various molecules in a wide variety of zeolites,[44–48] and in the interpretation of intensities of infrared bands of small molecules adsorbed in zeolite Na*A* and Ca*A*,[49–52] does not work for shielding. We consider this further in the Discussion.

If we assume that the $\sigma(^{39}\mathrm{Ar}, \mathrm{Ar}\cdots\mathrm{O}_{\mathrm{zeol}})$ function is the same for all *A*-type frameworks with Al/Si ratio=1.0, then the fitting of all the *ab initio* values for the Na*A*, K*A*, and Ca*A* zeolite fragments together leads to the shielding functions $\sigma(^{39}\mathrm{Ar}, \mathrm{Ar}\cdots\mathrm{Na}_{\mathrm{zeol}})$, $\sigma(^{39}\mathrm{Ar}, \mathrm{Ar}\cdots\mathrm{K}_{\mathrm{zeol}})$, and $\sigma(^{39}\mathrm{Ar}, \mathrm{Ar}\cdots\mathrm{Ca}_{\mathrm{zeol}})$, which are shown in Fig. 7. The deshielding contribution at the ^{39}Ar nucleus from a counterion is clearly a

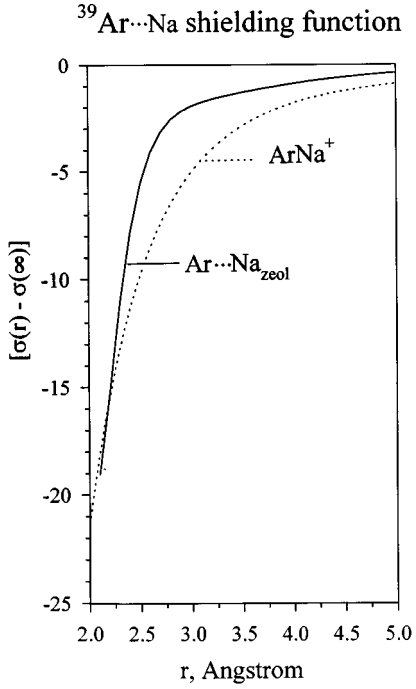

FIG. 6. The Na contribution to the pairwise additive shielding function of an ^{39}Ar nucleus in an Ar atom in the presence of the zeolite cage $\sigma(^{39}\text{Ar}, \text{Ar}\cdots\text{Na}_{zeol})$ is compared to the previously published shielding in the $\text{Ar}\cdots\text{Na}^+$ system where an Ar atom is interacting only with a bare Na^+ ion (Ref. 20). The long tail of the Ar shielding in the presence of the bare Na^+ ion is not found in the ^{39}Ar shielding of the Ar···zeolite fragment.

function of the number of electrons on the ion. The deshielding due to the Na in the zeolite is much less than that due to K at the same distance, and Ca is intermediate. The Ca contribution to the ^{39}Ar shielding has a longer tail than the K contribution to the shielding and similar to the previously published $\text{Ar}-\text{Na}^+$ shielding function, which may be due to its multiple charge. From these results alone, it may be possible to surmise, without doing the proper averaging, that the chemical shift of the single Xe trapped in the alpha cage of zeolite K*A* would be greater than the chemical shift of the single Xe in the alpha cage of Na*A*. The experimental data, obtained in our laboratory and reported elsewhere indeed shows that the single Xe in the K*A* alpha cage has a chemical shift which is 4 ppm greater than that which has been observed for a single Xe in the alpha cage of Na*A*.[26] We also tried fitting to the *ab initio* shielding values of the Na*A* zeolite fragments separately from the K*A* zeolite fragments. We find that the $\sigma(^{39}\text{Ar},\text{Ar}\cdots\text{O}_{zeol})$ function that we get from the separate fittings is nearly the same, differing from the each other by no more than 1–2 ppm at some points, supporting our assumption that it would appropriate to fit the Na*A* and K*A* fragments together. The size of the cations and its influence on the shielding function is obvious in Fig. 7. Eventually, it may be possible to express all rare gas···cation (-in-zeolite) shielding functions to a universal reduced form, using a distance scaled according to some distance parameter (e.g., r_0) of the potential function, for monovalent cations, with di- and trivalent cations considered separately. That will be considered at a later time.

It has been determined experimentally that the Xe in the limit of zero coverage in Ca*A* has a greater chemical shift than a single Xe in Na*A*.[53] While a proper averaging of the Xe positions in Ca*A* and the shielding functions $\sigma(^{129}\text{Xe}, \text{Xe}\cdots\text{Ca}_{zeol})$ and $\sigma(^{39}\text{Ar}, \text{Ar}\cdots\text{O}_{zeol})$ has yet to be carried out, the differences between the $\sigma(^{39}\text{Ar}, \text{Ar}\cdots\text{Na}_{zeol})$, $\sigma(^{39}\text{Ar}, \text{Ar}\cdots\text{K}_{zeol})$, and $\sigma(^{39}\text{Ar}, \text{Ar}\cdots\text{Ca}_{zeol})$ functions shown in Fig. 7 provide some support that the experimental trend can be reproduced.

We will present in a subsequent paper the grand canonical Monte Carlo (GCMC) simulations using the shielding functions derived here for ^{39}Ar, scaled to ^{129}Xe, to find the ^{129}Xe chemical shift of a single Xe atom in Na*A*, K*A*, and Ca*A* zeolites. The question yet remains, of course, as to whether the $\sigma(^{39}\text{Ar}, \text{Ar}\cdots\text{O}_{zeol})$ shielding function is universal for zeolites with Al/Si ratio=1.0, whether they be type *A*, faujasite, or other zeolite frameworks.

The dependence of the ^{39}Ar shielding on the Al/Si ratio of the zeolite fragment

We next consider the dependence of the shielding of the rare gas atom on the Al/Si ratio of the zeolite. This is of considerable interest because Xe NMR chemical shifts have been used empirically to characterize dealumination of zeolites. There are experimental data in the literature on Xe chemical shifts in Na*Y* vs Na*X*, for example. There have been many questions as to where the Al substitution sites are in various samples of these faujasites, as the Al/Si ratio goes from 0.0.018 to 0.8, for example.[11] The x-ray data from different laboratories are not in agreement about the details of the structure, even where the Na ions are.[54–59] The differing

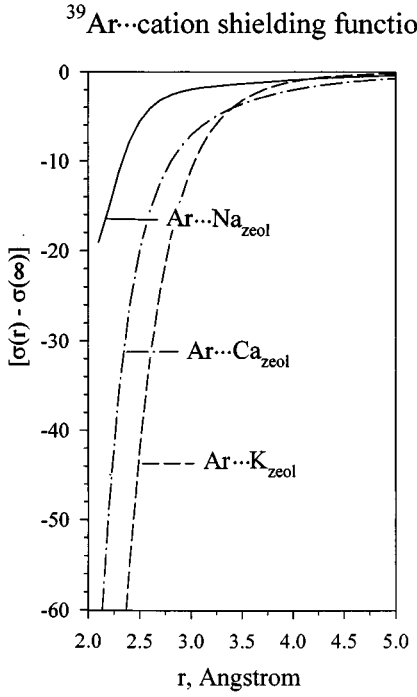

FIG. 7. The shielding functions $\sigma(^{39}\text{Ar}, \text{Ar}\cdots\text{Na}_{zeol})$, $\sigma(^{39}\text{Ar}, \text{Ar}\cdots\text{K}_{zeol})$, and $\sigma(^{39}\text{Ar}, \text{Ar}\cdots\text{Ca}_{zeol})$ obtained by fitting of all the *ab initio* values for Ar atom with the Na*A*, K*A*, and Ca*A* zeolite fragments taken together. The deshielding contribution at the ^{39}Ar nucleus from a counter-ion is clearly a function of the number of electrons on the ion.

TABLE I. ^{39}Ar intermolecular shielding (in ppm) of Ar atom in the presence of a 6-ring fragment with various Al/Si ratios, from GIAO calculations on neutral clusters $[Si_6O_6(OH)_{12}]$, $[Si_5AlO_6(OH)_{12}]^-$ Na^+, $[Si_4Al_2O_6(OH)_{12}]^{2-}$ Na_2^+ and $[Si_3Al_3O_6(OH)_{12}]^{3-}$ Na_3^+, with Al/Si=0, 0.2, 0.5, 1.0, respectively. The Roman numerals designate the site type, the asterisks denote the values plotted in Fig. 8 and the distances given are between the Ar and Na or O atoms specifically labeled (a–f) in the fragment in Fig. 2. In the table heading the subscripts a–f correspond to the labels for the O atoms above which the Ar is placed.

Al/Si	Na(I)	$O(I)_a$*	$O(I)_b$	$O(I)_c$	$O(II)_d$	$O(II)_e$*	$O(II)_f$
			2.5 Å				
0.0	−10.7	−68.04	−68.04	−68.04	−75.28	−75.28	−75.28
0.2	−16.87	−74.41	−70.45	−70.74	−78.82	−79.15	
0.5	−20.79	−78.40			−80.76	−79.09	
1.0	−22.79	−81.45	−74.47			−79.58	
			3.0 Å				
0.0	−3.95	−25.90	−25.90	−25.90	−29.46	−29.46	−29.46
0.2	−5.40	−31.04	−26.40	−26.85	−30.74	−30.67	
0.5	−8.07	−34.23	−31.93		−35.15	−31.43	
1.0	−9.48	−34.52	−32.28		−35.10	−34.80	
			4.0 Å				
0.0		−2.90	−2.90	−2.90	−3.38	−3.38	−3.38
0.2	−0.53	−4.61	−2.63	−2.82	−3.28	−3.14	
0.5	−1.42	−4.90	−4.98	−3.85	−5.59	−3.56	
1.0	−2.02	−5.27	−5.37		−5.90	−5.47	

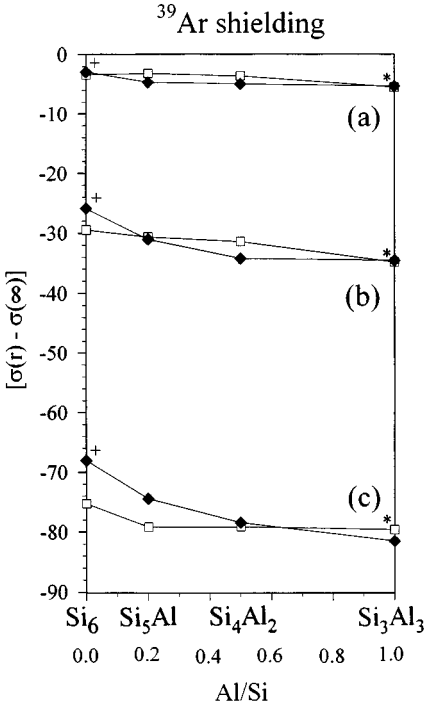

FIG. 8. The *ab initio* values of the ^{39}Ar shielding in an Ar atom at three different positions (a) 4.0 Å, (b) 3.0 Å, and (c) 2.5 Å above an O atom in the 6-ring fragment in Fig. 2, in which the Al/Si ratio changes upon replacement of the Si with Al. Calculations were carried out on the neutral fragments $[Si_6O_6(OH)_{12}]$, $[Si_5AlO_6(OH)_{12}]^-$ Na^+, $[Si_4Al_2O_6(OH)_{12}]^{2-}$ Na_2^+ and $[Si_3Al_3O_6(OH)_{12}]^{3-}$ Na_3^+. The *ab initio* values shown are for the Ar atom located above a bridging O(I) atom O_a(◆), where the O(I) in this plot is a SiOAl bridge, except where marked with a +, at which point the last Al has been changed into an Si. The other set of *ab initio* values shown are for the Ar atom located above another bridging O(II) atom O_e(□), where the O(II) in this plot is a SiOSi bridge, except where marked with an asterisk *, at which point it becomes a SiOAl bridge.

Xe chemical shifts in Na*Y* vs Na*X* may be in part due to the different averaging that takes place for Xe within these faujasites, as may be surmised from the change in the adsorption isotherm with Al/Si ratio.[44] Such changes are also well documented in silicalite versus ZSM-5.[21] On the other hand, the chemical shift function may itself be different when the Al/Si ratio of the zeolite changes. In order to separately answer these two questions, we examine here the dependence of the Ar shielding on the Al/Si ratio of the zeolite fragment. In these calculations, we only constructed fragments which have fewer Al atoms than the *A*-type fragments shown in Figs. 1–3. We kept the geometries identical to the *A*-type fragments in order to obtain only the effect of changing the Al/Si ratio, without changing the structure. The number of *ab initio* calculations for this study are not as large as those used for the determination of the Ar shielding function in the Al/Si=1.0 case, but the trends are quite clear. The specific results for the six-ring fragment are shown in Table I. Here, the shieldings are calculated for the structure shown in Fig. 2, without relaxing the geometry as each of the Al and Na pairs are successively replaced by an Si atom. We present in Table I some of the actual *ab initio* values at various positions of the Ar relative to the 6-ring fragment in Figs. 8 and 9. Several interesting points should be noted here: The effect of changing the Al/Si ratio is great at short distances, and not as pronounced at longer distances. Nevertheless, the trend is unequivocal, *the* ^{39}*Ar nucleus is more deshielded when the Al/Si ratio is larger*. The ^{39}Ar shielding values calculated for Ar locations directly above a Na^+ ion are not as deshielding as when the Ar is located at the same distance directly above an O atom, but the percent change with changing Al/Si ratio is greater for the former. Shielding is a highly local property, as we can see from the dramatic distance dependence in Figs. 5–7. Therefore, it is not surprising that the change is small as the overall number of Al content of the zeolite fragment is changed, but it is rather dramatic when the Al or Si attached to O atom closest to the Ar is itself substituted. Likewise, there is a small shielding change at the Ar placed above a Na^+ ion as the Al content of the zeolite fragment is changed, but there is a dramatic change when the Na^+ ion closest to the Ar is itself removed. Finally, it is important to note that the changes are more pronounced when the Ar is placed above an O atom than above a Na^+ ion.

The dependence of the ^{129}Xe chemical shift on the Al/Si ratio of the zeolite in which it is adsorbed has been discussed by several authors, but there are a limited number of unequivocal examples. One is the ca. 4 ppm difference between Xe chemical shifts in the limit of zero loading for zeolite Na*Y* through Na*X* (the latter has a much higher number of Al substituting for Si in the faujasite-type lattice), with the Al/Si ratio ranging from 0.018 to 0.8,[11] and the other is the systematic change in Xe chemical shifts in the limit of zero loading for silicalite (the purely Si version of the MFI-type zeolite called ZSM-5) to ZSM-5 at various Al/Si ratios, not including the change accompanying the phase transition, as the number of Al atoms varies from 0 up to 2 per unit cell.[21] These examples establish that the ^{129}Xe chemical shift in the

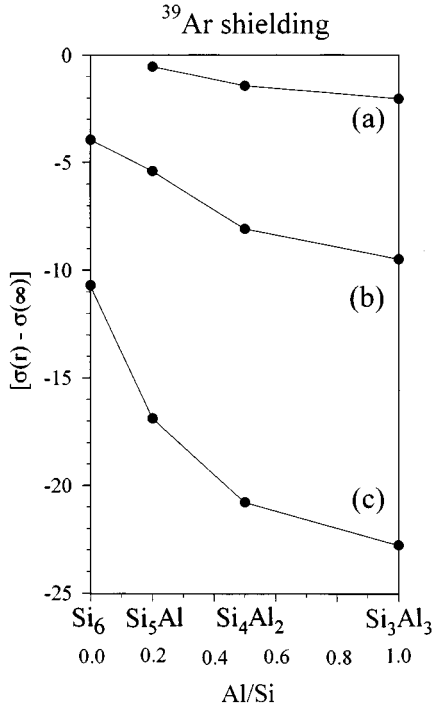

FIG. 9. The *ab initio* values of the ^{39}Ar shielding in an Ar atom at three different positions (a) 4.0 Å, (b) 3.0 Å, and (c) 2.5 Å above the Na(I) in the center of the 6-ring fragment in Fig. 2, in which the Al/Si ratio changes upon replacement of the Si with Al. Calculations were carried out on the neutral fragments $[Si_6O_6(OH)_{12}]$, $[Si_5AlO_6(OH)_{12}]^-$ Na^+, $[Si_4Al_2O_6(OH)_{12}]^{2-}$ Na_2^+ and $[Si_3Al_3O_6(OH)_{12}]^{3-}$ Na_3^+. The much smaller deshielding at the [Al]/[Si]=0 corresponds to the loss of the Na ion just below the Ar atom.

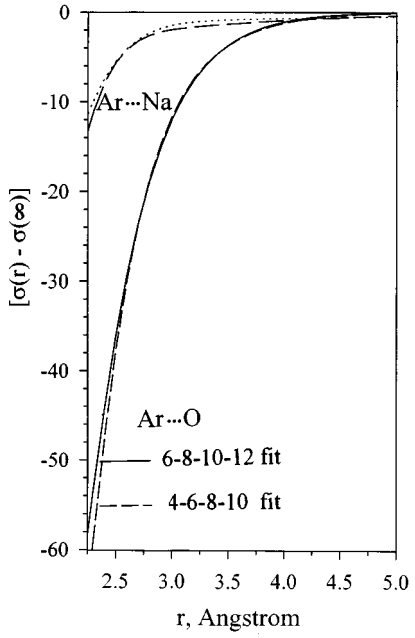

FIG. 10. The functional form for fitting the *ab initio* shielding values for ^{39}Ar shielding in the presence of a zeolite fragment influences the partitioning of the shielding into contributions from O atoms and from Na^+ ions. The fits using exponents $-4,-6,-8,-10$ are here compared with the fit using $-6,-8,-10,-12$ described in the text.

limit of zero loading increases with increasing Al content, all other factors being the same. The accompanying increase in the adsorption enthalpies and increase in Henry's law constant found with increasing Al content in these zeolites[21,44] indicates that greater attractive interactions between the rare gas atoms and the zeolites with increasing Al content affect the ^{129}Xe chemical shift averaging process, that is, if the function describing the shielding response of the Xe to the zeolite is unchanged upon changing the Al/Si ratio, the change in the averaging upon changing the Al/Si ratio may itself give rise to larger Xe chemical shifts with increasing Al content. On the other hand, our *ab initio* calculations of the shielding of a rare gas atom in the presence of zeolite fragments with changing number of Al-for-Si substitutions unequivocally find that the rare gas atom chemical shift should increase with increasing Al content, due to changes in the shielding function alone, even without any changes in the averaging over configurations.

One of the questions we have not yet addressed is the sensitivity of the partitioning of the framework contributions $\sigma(^{39}\mathrm{Ar,Ar}\cdots\mathrm{O_{zeol}})$ and the cation contributions $\sigma(^{39}\mathrm{Ar,Ar}\cdots\mathrm{Na_{zeol}})$ to the form of the functions used for fitting. The functions in the inverse powers of the Ar···O and Ar···Na^+ distances that we used are based on the previous findings of the distance dependence of the shielding in pairs of rare gas atoms such as Ne–He, Ne–Ne, Ar–Ne, Ar–Ar, as well as rare gas atoms interacting with small molecules such as OH_2 and NaH and Na^+ ion.[20,42] In these simple systems the functional form of the distance dependence could be explored by making a logarithmic plot. In these examples, the slopes found ranged from -3.44 for Ar···Na^+ to -4.94 for Ar···NaH while the rare gas pairs gave slopes of -6.67, -6.79, -6.74, -7.41. Thus we started fitting to linear combinations of inverse powers such as -4, -6, -8, -10 of the Ar···O distance. In Fig. 10 we compare the results of fitting the *ab initio* values of the Ar shielding in the presence of the zeolite fragments to two different functional forms, where the same functional form is used for both the O atom and the cation contributions. We see that the functional form used for fitting does influence, but only slightly, how much of the shielding is attributed to O atoms and how much to the cations. We have reported in Figs. 5 and 6 the fit corresponding to the smallest overall variance: the form

$$\sigma(^{39}\mathrm{Ar,Ar}\cdots\mathrm{O_{zeol}}) = a_6 r^{-6} + a_8 r^{-8} + a_{10} r^{-10} + a_{12} r^{-12}$$

for O atoms, and the identical form for the cations. The grand canonical average chemical shifts of Xe in various zeolites containing Na, K, and Ca ions could result in different results from using the two functional forms and may reveal which one provides a more realistic partitioning of the contributions from cations and O atoms.

The anisotropy of the shielding of a rare gas atom in a zeolite

A very interesting aspect of the intermolecular shielding of ^{129}Xe in a microporous solid is its anisotropy. This has been the subject of several investigations of immobilized Xe line shapes at low temperatures.[60–62] It was originally proposed that the shape of the cavity in which the Xe atom finds itself was the determining factor for the anisotropy, that the

TABLE II. Shielding tensor components (ppm) for ^{39}Ar in an Ar atom located at various positions relative to the zeolite 6-ring fragment $[Si_3Al_3O_6(OH)_{12}]^{3-}$ Na_3^+, and the 8-ring fragment $[Si_4Al_4O_8(OH)_{16}]^{4-}$ Na_4^+ shown in Figs. 2 and 3. The Roman numerals designate the site type for the Na ion.

Å	σ_{11}	σ_{22}	σ_{33}	σ_{iso}[a]	σ_{aniso}[b]	η[c]
			8-ring			
r(Ar–Na^{II})						
2.5	−23.3	−22.4	−7.5	−17.7	15.4	.06
3.0	−8.9	−6.4	−1.5	−5.6	6.1	.41
4.0	−1.8	−0.9	0.8	−0.6	2.2	.41
5.0	−0.9	−0.8	1.2	−0.2	2.1	.06
r(Ar–O)						
2.5	−152.5	−115.9	−88.9	−119.1	45.3	.81
3.0	−78.5	−58.5	−35.8	−57.6	32.7	.61
4.0	−14.0	−10.7	−2.0	−8.9	10.4	.31
5.0	−2.2	−1.4	1.7	−0.7	3.5	.24
			6-ring			
r(Ar–Na^{I})						
2.5	−23.7	−23.4	−5.0	−17.4	18.5	.02
3.0	−8.7	−8.5	0.1	−5.7	8.7	.03
4.0	−2.3	−2.2	2.0	−0.8	4.2	.02
5.0	−1.4	−1.4	1.9	−0.3	3.2	.00
r(Ar–O)						
2.5	−100.3	−74.5	−34.2	−69.7	53.2	.48
3.0	−39.3	−31.9	−12.8	−28.0	22.9	.32
4.0	−6.7	−6.1	0.9	−4.0	7.3	.09
5.0	−2.0	−1.8	1.9	−0.6	3.8	.06
r(Ar–O)						
2.5	−104.4	−86.9	−41.3	−77.6	54.3	.32
3.0	−42.7	−39.4	−15.5	−32.5	25.5	.13
4.0	−8.2	−6.7	0.6	−4.8	8.1	.18
5.0	−2.3	−1.8	1.9	−0.7	4.0	.11

[a] $\sigma_{iso}=(\sigma_{11}+\sigma_{22}+\sigma_{33})/3$.
[b] $\sigma_{aniso}=\sigma_{33}-(\sigma_{11}+\sigma_{22})/2$.
[c] $\eta=(\sigma_{22}-\sigma_{11})/\sigma_{aniso}$.

Xe electron cloud is molded by the shape of the channel.[60] This can not be the case except perhaps for a cavity which in a space-filling model leaves a void just barely the size of a single Xe atom. A different explanation has been offered for the line shapes of Xe in these early examples: that a Xe atom static at a site on the pore wall has an axially symmetric shielding tensor with the principal axis normal to the wall, so that the line shape observed reflects the distribution of orientations of such axes in a cylindrical pore.[61] In a recent study, the anisotropic line shapes of Xe shielding in AlPO-11 as a function of loading has been interpreted in terms of three Xe sites, each one having its own anisotropic shielding tensor, and these tensor components have been obtained from experiment.[62] The rather large anisotropies of the three Xe shielding tensors in this example are very interesting and can be calculated by the same method applied here, except that instead of zeolite fragments containing Si–O–Al and cations, we would use fragments containing P–O–Al.

Let us we now examine the anisotropy of the rare gas atom shielding tensors that we have calculated. We have a wealth of anisotropy information in the 164 *ab initio* shielding tensors for Ar in the presence of fragments of Na*A*, K*A*, and Ca*A*, as well as the siliceous versions of the 4- and 6-ring fragments. We present only a few examples here to provide some insight. Table II presents the tensor characteristics of ^{39}Ar shielding at various positions relative to a 6-ring fragment and an 8-ring fragment, with the Ar located 2.5 to 5.0 Å above Na(I), Na(II), and three types of O atoms. The Na(I) ion in the 6-ring is in the most symmetrical position as can be seen in Fig. 2. Therefore it is not surprising that the Ar shielding tensor is essentially axially symmetric when the Ar is placed above this Na(I) at all distances. The Na(II) in the 8-ring is located off-center in the ring, coordinated to three oxygens, leading to substantial asymmetry in the Ar shielding except at very close distances, where the Ar is so close to the Na(II) that the contributions from the rest of the fragment become unimportant, or at very large distances where the off-center aspect of the Na(II) location also becomes unimportant, in which cases the tensor is nearly axial. Contrary to what was suggested earlier,[61] the shielding tensor of a rare gas atom on the inside wall of a zeolite cavity is hardly axially symmetric.[62] An even better indication of the lineshape than the standard definition of the anisotropy $\sigma_{aniso}=\sigma_{33}-(\sigma_{11}+\sigma_{22})/2$, is the span $(\sigma_{33}-\sigma_{11})$ which gives the spread of the signal in ppm in the NMR spectrum of the powder at low temperatures. For the sites shown in Table II, these are larger than σ_{aniso} when the tensor is not axially symmetric, ranging from 4–66 ppm for positions above the O atoms and 2–18.7 ppm for positions above the Na ions. The corresponding values would be a factor of roughly four times as large when scaled up to Xe shielding at these positions. Indeed, the observed line shapes for Xe in AlPO-11 are not axially symmetric and have spans of 55.3 up to 90.9 ppm depending on the number of nearest Xe neighbors (0–2) at the site.[62]

CONCLUSIONS

We have determined the average effective shielding of the ^{39}Ar nucleus in an argon atom in Na*A*, K*A*, and Ca*A* zeolite cages modeled by neutral 4-ring, 6-ring, and 8-ring fragments. The entire isotropic shielding obtained by *ab initio* calculations using the GIAO method is assumed to be expressed as a sum over pairwise additive isotropic shielding functions $\sigma(^{39}\text{Ar, Ar}\cdots\text{O}_{zeol})$ and $\sigma(^{39}\text{Ar, Ar}\cdots\text{Na}_{zeol})$ for the intermolecular effects of the Ar interactions with oxygen atoms of the zeolite framework and the Na^+ counterions, and the shielding functions are taken to be of the form of a simple four-term linear combination in inverse powers of the Ar–O and Ar–Na distances respectively. In the same way, the shielding functions $\sigma(^{39}\text{Ar, Ar}\cdots\text{K}_{zeol})$ and $\sigma(^{39}\text{Ar, Ar}\cdots\text{Ca}_{zeol})$ are obtained. The expected trends with respect to the size and polarizability of the cation are found: The deshielding of the ^{39}Ar in the Ar atom is greatest for interaction with the largest and the most polarizable cations. The dependence of the ^{39}Ar shielding on the Al/Si ratio of the zeolite fragment has been established in this work: At the same position of the Ar relative to the zeolite, the deshielding effect of the intermolecular interaction increases with Al content. The results are in agreement with the few experimental cases where the dependence of the ^{129}Xe chemical shift on the Al/Si ratio of the zeolite has been observed. The magnitudes of the anisotropies of the intermolecular shielding ten-

sors found here are consistent with the observed line shapes in the powder spectra of immobilized Xe in zeolite pores.

ACKNOWLEDGMENTS

This research was supported by The National Science Foundation (Grant No. CHE92-10790). We are grateful to Peter Pulay for providing us with a copy of the code for TX90 with which all the calculations described in this paper were carried out. We thank Angel C. de Dios for enlightening discussions and consultations regarding the use of the TX90 program.

[1] J. Fraissard and T. Ito, Zeolites **8**, 350 (1988).
[2] C. Dybowski, N. Bansal, and T. M. Duncan, Ann. Rev. Phys. Chem. **42**, 433 (1991).
[3] P. J. Barrie and J. Klinowski, Prog. NMR Spectrosc. **24**, 91 (1992).
[4] T. R. Stengle and K. L. Williamson, Macromolecules **20**, 1428 (1987).
[5] J. B. Miller, J. H. Walton, and C. M. Roland, Macromolecules **26**, 5602 (1993).
[6] A. P. M. Kentgens, H. A. van Boxtel, R. J. Verweel, and W. S. Veeman, Macromolecules **24**, 3712 (1991).
[7] G. Neue, Z. Phys. Chem. **152**, 27 (1987).
[8] D. J. Suh, T. J. Park, S. K. Ihm, and R. Ryoo, J. Phys. Chem. **95**, 3767 (1991).
[9] J. A. Ripmeester, J. S. Tse, C. I. Ratcliffe, and B. M. Powell, Nature (London) **325**, 135 (1987).
[10] P. J. Barrie, G. F. McCann, I. Gameson, T. Rayment, and J. Klinowski, J. Phys. Chem. **95**, 9416 (1991).
[11] J. Fraissard and T. Ito, J. Chem. Phys. **76**, 5225 (1982).
[12] E. G. Derouane and J. B. Nagy, Chem. Phys. Lett. **137**, 341 (1987).
[13] J. Demarquay and J. Fraissard, Chem. Phys. Lett. **136**, 314 (1987).
[14] D. W. Johnson and L. Griffiths, Zeolites **7**, 484 (1987).
[15] J. A. Ripmeester, C. I. Ratcliffe, and J. S. Tse, J. Chem. Soc., Faraday Trans. 1 **84**, 3731 (1988).
[16] S. B. Liu, B. M. Fung, T. C. Yang, E. C. Hong, C. T. Chang, P. C. Shih, F. H. Tong, and T. L. Chen, J. Phys. Chem. **98**, 4393 (1994).
[17] B. Boddenberg and M. Hartmann, Chem. Phys. Lett. **203**, 243 (1993).
[18] L. C. de Menorval, J. Fraissard, and T. Ito, J. Chem. Soc., Faraday Trans. 1 **78**, 403 (1982).
[19] C. J. Jameson, A. K. Jameson, B. I. Baello, and H. M. Lim, J. Chem. Phys. **100**, 5965 (1994).
[20] C. J. Jameson and A. C. de Dios, J. Chem. Phys. **97**, 417 (1992).
[21] Q. Chen, M. A. Springel-Huet, J. Fraissard, M. L. Smith, D. R. Corbin, and C. Dybowski, J. Phys. Chem. **96**, 10914 (1992).
[22] J. J. Pluth and J. V. Smith, J. Am. Chem. Soc. **102**, 4704 (1980).
[23] J. J. Pluth and J. V. Smith, J. Phys. Chem. **83**, 741 (1979).
[24] J. J. Pluth and J. V. Smith, in *ACS Symposium Series*, edited by G. D. Stucky and F. G. Dwyer (American Chemical Society, Washington, D.C., 1983), Vol. 218; J. Am. Chem. Soc. **105**, 1192 (1983).
[25] C. J. Jameson, A. K. Jameson, R. E. Gerald II, and A. C. de Dios, J. Chem. Phys. **96**, 1676 (1992).
[26] C. J. Jameson, A. K. Jameson, R. E. Gerald II, and H. M. Lim, J. Chem. Phys. (to be published).
[27] *Nuclear Magnetic Shieldings and Molecular Structure*, edited by J. A. Tossell, NATO ASI Series C Vol. 386 (Kluwer, Dordrecht, 1993).
[28] M. Schindler and W. Kutzelnigg, J. Chem. Phys. **76**, 1919 (1982).
[29] W. Kutzelnigg, M. Schindler, and U. Fleischer, *NMR Basic Principles and Progress* (Springer, Berlin, 1990), Vol. 23.
[30] A. E. Hansen and T. D. Bouman, J. Chem. Phys. **82**, 5035 (1985).
[31] R. Ditchfield, Mol. Phys. **27**, 789 (1974).
[32] K. Wolinski, J. Hinton, and P. Pulay, J. Am. Chem. Soc. **112**, 8251 (1990).
[33] C. J. Jameson, B. I. Baello, and H. M. Lim (unpublished results).
[34] TEXAS, P. Pulay, 1991, The University of Arkansas, Fayetteville, Arkansas 72701.
[35] P. Pulay, J. F. Hinton, and K. Wolinski, in *Nuclear Magnetic Shieldings and Molecular Structure*, edited by J. A. Tossell, NATO ASI Series C, Vol. 386 (Kluwer, Dordrecht, 1993), p. 243–262.
[36] S. Huzinaga, *Gaussian Basis Sets for Molecular Calculations* (Elsevier, Amsterdam, 1984).
[37] D. B. Chesnut and K. D. Moore, J. Comput. Chem. **10**, 648 (1989).
[38] D. B. Chesnut, B. E. Rusiloski, K. D. Moore, and D. A. Egolf, J. Comput. Chem. **14**, 1364 (1993).
[39] J. H. vanLenthe, J. G. C. M. van Duijneveldt-van de Rijdt, and F. B. van Duijneveldt, Adv. Chem. Phys. **69**, 521 (1987).
[40] G. Chalasinski and M. Gutowski, Chem. Rev. **88**, 943 (1988).
[41] S. F. Boys and F. Bernardi, Mol. Phys. **19**, 538 (1970).
[42] C. J. Jameson and A. C. de Dios, J. Chem. Phys. **98**, 2208 (1993).
[43] C. J. Jameson and A. C. de Dios, in *Nuclear Magnetic Shieldings and Molecular Structure*, edited by J. A. Tossell, NATO ASI Series C, Vol. 386 (Kluwer, Dordrecht, 1993), p. 95–116.
[44] A. V. Kiselev and P. Q. Du, J. Chem. Soc. Faraday Trans. 2 **77**, 1 (1981).
[45] A. G. Bezus, M. Kocirik, and E. A. Vasilyeva, Zeolites **7**, 327 (1987).
[46] T. Yamazaki, S. Ozawa, and Y. Ogino, Mol. Phys. **69**, 369 (1990).
[47] L. Uytterhoeven, D. Dompas, and W. J. Mortier, J. Chem. Soc. Faraday Trans. **88**, 2753 (1992).
[48] E. Cohen de Lara and T. N. Tan, J. Phys. Chem. **80**, 917 (1976).
[49] E. Cohen de Lara and J. Vincent-Geisse, J. Phys. Chem. **80**, 1922 (1976).
[50] E. Cohen de Lara, R. Kahn, and A. M. Goulay, J. Phys. Chem. **90**, 7482 (1989).
[51] E. Cohen de Lara, A. M. Goulay, J. Soussen-Jacob, and R. Kahn, Mol. Phys. **76**, 1049 (1992).
[52] A. V. Larin, F. Jousse, and E. Cohen de Lara, in *Zeolites and Related Microporous Materials: State of the Art 1994*, edited by J. Weitkamp, H. G. Karge, H. Pfeifer, and W. Holderich (Elsevier, Amsterdam, 1994) p. 2147.
[53] C. J. Jameson, A. K. Jameson, R. E. Gerald II, and A. C. de Dios, J. Chem. Phys. **96**, 1690 (1992).
[54] D. H. Olson, J. Phys. Chem. **74**, 2758 (1970).
[55] M. Eddy, D. Philos. thesis, Oxford University, 1985.
[56] W. J. Mortier, E. van den Bossche, and L. Uytterhoeven, Zeolites **4**, 41 (1984).
[57] G. R. Eulenberger, D. P. Shoemaker, and J. G. Keil, J. Phys. Chem. **71**, 1812 (1967).
[58] A. N. Fitch, H. Jobic, and A. Renouprez, J. Phys. Chem. **90**, 1311 (1986).
[59] Z. A. Kaszkur, R. H. Jones, D. Waller, C. R. A. Catlow, and J. M. Thomas, J. Phys. Chem. **97**, 426 (1993).
[60] M. A. Springuel-Huet and J. Fraissard, Chem. Phys. Lett. **154**, 299 (1989).
[61] J. A. Ripmeester, C. I. Ratcliffe, and J. S. Tse, J. Chem. Soc., Faraday Trans. 1 **84**, 3731 (1988).
[62] J. A. Ripmeester and C. I. Ratcliffe, J. Phys. Chem. **99**, 619 (1995).